ELSEVIER

Bone 38 (2006) 722 – 730

BONE

www.elsevier.com/locate/bone

Geometry and cell density of rat craniofacial sutures during early postnatal development and upon in vivo cyclic loading

Kapil Vij, Jeremy J. Mao *

Tissue Engineering Laboratory, University of Illinois at Chicago MC 841, 801 South Paulina Street, Chicago, IL 60612-7211, USA

Received 29 July 2005; revised 7 October 2005; accepted 11 October 2005
Available online 18 January 2006

Abstract

Cranial sutures are unique to skull bones and consist of multiple connective tissue cell lineages such as mesenchymal cells, fibroblast-like cells, and osteogenic cells, in addition to osteoclasts. Mechanical modulation of intramembranous bone growth in the craniofacial suture is not well understood, especially during postnatal development. This study investigated whether in vivo mechanical forces regulate sutural growth responses in postnatal rats. Cyclic compressive forces with a peak-to-peak magnitude of 300 mN and 4 Hz were applied to the maxilla in each of 17-, 23-and 32-day-old rats for 20 min/day over 5 consecutive days. Computerized histomorphometric analysis revealed that cyclic loading significantly increased the average geometric widths of the premaxillomaxillary suture (PMS) to 86 ± 7 μm, 99 ± 12 μm, and 149 ± 30 μm, representing 32%, 50%, and 39% increases for P17, P23, and P32 in comparison with age-matched sham controls. For the nasofrontal suture (NFS), cyclic loading significantly increased the average sutural widths to 88 ± 15 μm, 92 ± 10 μm, and 100 ± 14 μm, representing 33%, 24%, and 32% increases for P17, P23, and P32 relative to age-matched controls. The average PMS cell density upon cyclic loading was 10182 ± 132 cells/mm^2, 9752 ± 661 cells/mm^2, and 9521 ± 628 cells/mm^2, representing 62%, 35%, and 30% increases for P17, P23, and P32 in comparison with age-matched controls. For the NFS, cyclic loading increased the average cell density to 9884 ± 893 cells/mm^2, 9818 ± 1091 cells/mm^2, 9355 ± 661 cells/mm^2, representing 44%, 46% and 40% increases at P17, P23, and P32 respectively. Osteoblast-occupied sutural bone surface was significantly greater in cyclically loaded sutures for P17, P23, and P32 than corresponding controls for both the PMS and NFS. On the other hand, cyclic loading elicited significantly higher sutural bone surface populated by osteoclast-like cells by P17 and P23 days, but not P32 days, for the PMS. For the NFS, sutural osteoclast surface was significantly higher upon cyclic loading for P23 and P32 days, but not P17. The present data demonstrate that cyclic forces are potent stimuli for modulating postnatal sutural development, potentially by stimulating both osteogenesis and osteoclastogenesis. Cyclic loading may have clinical implications as novel mechanical stimuli for modulating craniofacial growth in patients suffering from craniofacial anomalies and dentofacial deformities.

Keywords: Sutures; Forces; Osteogenesis; Fibroblasts; Osteoblasts

Introduction

Whereas appendicular bones lengthen by endochondral ossification of growth plates, most craniofacial bones elongate by intramembranous bone apposition in craniofacial sutures. Sutures are unique to skull bones and consist of multiple cell lineages such as mesenchymal cells, fibroblast-like cells and osteogenic cells [1–3]. During active growth, sutural osteoblasts continue to lay down bone matrix, whereas sutural fibroblast-like cells synthesize non-mineralized matrices with a net result of continuous maintenance of the presence of sutures [1–4]. Osteoclasts are increasingly demonstrated to play important roles in the development of both normal and synostosed cranial sutures [5–8]. Although the exact lineages of sutural cells are not fully understood, it is clear that cranial sutures must be patent for cranial vault bones to lengthen [1–3]. Thus, the geometry of cranial sutures is a physical parameter of considerable importance for understanding sutural growth, perhaps analogous to the importance of the height of growth plate in the longitudinal growth of appendicular bones. Previously, two amalgam markers have been implanted across a given location of a cranial suture to measure sutural width changes over time [9,10]. However, changes in the width of cranial sutures are not linear at

* Corresponding author. Fax: +1 312 996 7854.
E-mail address: jmao2@uic.edu (J.J. Mao).

8756-3282/$ - see front matter © 2005 Elsevier Inc. All rights reserved.
doi:10.1016/j.bone.2005.10.028

multiple locations [11,12]. Accordingly, it is desirable to measure sutural width along multiple locations of the sutural course so that comprehensive geometric changes in sutural width can be appreciated. This challenging aspect of sutural growth, in comparison with rather standardized measurements of growth plate height, has been tackled with the availability of computerized histomorphometry by quantifying multiple locations of sutural width [4,13]. Computerized histomorphometry has also allowed the quantification of the density of sutural cells [4]. Cell density represents another important determinant of sutural growth, given that sutural width changes are likely related to sutural cell proliferation and matrix synthesis [1–3].

Mechanical stress from functional activities such as mastication or upon exogenously applied mechanical forces modulates sutural growth [2,3,38]. Of particular interest is the observation of bone apposition and increases in sutural width in the craniofacial sutures under compressive strain [4,14,15]. Although it may seem no surprise to the orthopedic field that bone structures under compression increase bone apposition rates, the observed increases in sutural bone apposition in the craniofacial suture under compression are at variation with the generally accepted notion in craniofacial orthopedics that tension induces bone formation, whereas compression induces bone apposition [2]. Exogenous compressive forces against the rabbit maxilla in vivo induce compressive strain of the premaxillomaxillary suture, but tensile strain in the nasofrontal suture [13,16]. Yet, either exogenously induced sutural compression or sutural tension applied at 1 Hz for 10 min/day for 12 days has elicited growth responses in the rabbit premaxillomaxillary and nasofrontal sutures [4]. Matrix metalloproteinase genes 1 and 2 are expressed in postnatal cranial sutures both during normal postnatal development and upon cyclic loading [17–19]. The peak amplitude of cyclic mechanical strain that elicits sutural anabolic changes is considerably lower than peak strain used to induce anabolic changes in appendicular bones [2–4,18–24]. However, most of the previous work on mechanical modulation of bone growth in both appendicular and craniofacial skeletons has been performed in juvenile, skeletally immature animals. The goal of the present study was to determine whether exogenous cyclic forces delivered to craniofacial bones in postnatal rats elicit growth response in cranial sutures.

Material and methods

Animal model

Postnatal Sprague–Dawley rats with 17, 23, and 32 days of age (P17, P23, and P32) were used. These age groups were selected on the following basis. First, the rat posterior interfrontal suture is synostosed prior to P32, which likely has implications in the development of the rest of craniofacial sutures including those tested in this study. Second, we have previously investigated the expression of matrix metalloproteinase genes (MMPs) in craniofacial sutures at these age points [18,19], thus eliciting a continuing interest to investigate the presently studied morphological features of craniofacial sutures. For each age group, a total of 14 rats were randomly divided into the control group or mechanical loading group ($N = 7$ per group). The premaxillomaxillary suture (PMS) is shown in Fig. 1A and was selected due to its immediate adjacency to masticatory loading. The nasofrontal suture (NFS) is shown in Fig. 1B and was selected due to its relatively distant location from the point of masticatory loading.

Mechanical loading

Under general anesthesia by intramuscular injection of a cocktail containing 90% ketamine (100 mg/ml; Aveco, Ford Dodge, IA) and 10%

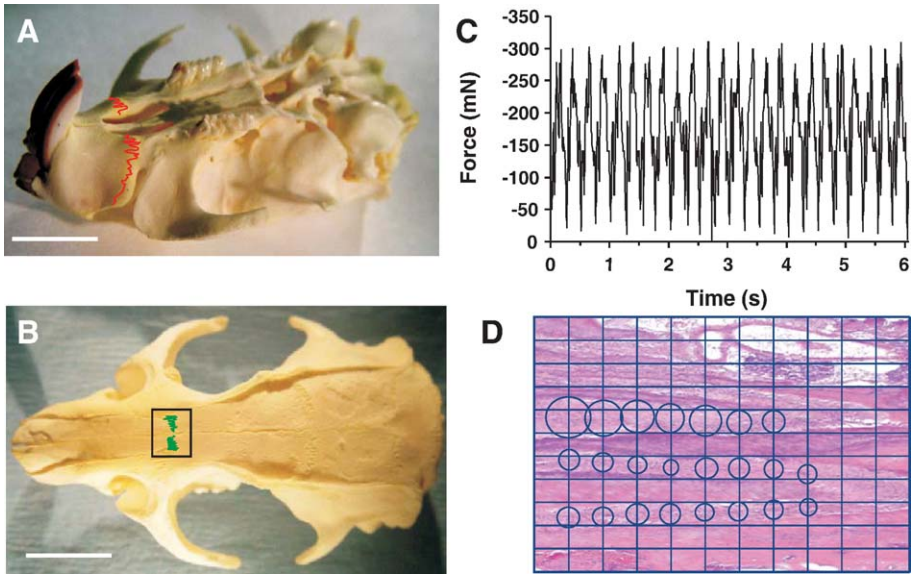

Fig. 1. Rat suture morphology, mechanical loading and quantification of sutural width. (A) Lateroventral view of the rat skull. The premaxillomaxillary suture is labeled as the red zig-zag line between the premaxilla in which the central incisors anchor, and the rest of the skull bones. Scale bar: 4 mm. (B) The superior view of the rat skull showing the nasofrontal suture in green and identified within a rectangular box. Scale bar: 4 mm. (C) Representative exogenous cyclic forces at 300 mN and 4 Hz applied to the rat maxilla showing 4 cycles of peak forces per second. The offset in the force chart is due to an initial baseline reading by the force sensor. (D) Histomorphometric measurements of sutural width by construction of grids over sutural microscopic specimen. The width of the suture at a given location is measured as the diameter of each of the circles that bisect the sutural width along each of the vertical lines of the grid.

xylazine (20 mg/ml; Mobay, Shawnee, KS), compressive forces with a peak magnitude of 300 mN and 4 Hz were programmed with a custom designed tissue loader [18,19] and delivered on the maxilla in vivo for 20 min/day over 5 consecutive days, leading to 4800 cycles per day (Fig. 1C). The rat in the cyclic loading group was placed in a supine position in a custom-made device that provided rigid fixation of the skull. The rat in the control group was subjected to general anesthesia and other manipulation with the exception of the application of mechanical loading. After daily experimental manipulation as described above, the rat recovered and resumed food intake. The rats were housed in a temperature-controlled room (23–25°C) and fed with standard amounts of food and water. The present animal protocol was approved by the institutional Animal Care Committee.

Tissue harvest and preparation

Following the last episode of mechanical loading on Day 5, the rats were euthanized by pentobarbital overdose. The premaxillomaxillary and nasofrontal sutures were dissected en bloc with at least 2 mm of surrounding bone. The specimens were trimmed, dehydrated and demineralized in 50% formic acid and 20% sodium citrate and embedded in paraffin blocks. Sequential 4–6 μm sections were cut in the parasagittal plane and stained with hematoxylin and eosin, and further used for histomorphometric measurements.

Computer-assisted histomorphometry

Quantitative histomorphometric analysis of sutural width and sutural cell density was performed by using a computerized image-analysis system. Standardized grids (110 × 110 μm^2) were constructed over sutural microscopic specimens under 10× magnification. The linear geometric width of the suture was measured by constructing circles that bisected the sutural width along the vertical grid lines (Fig. 1D). Each circle's diameter is equal to the width of the cranial suture at a given location. The total number of nucleated cells present in the suture, excluding those lining the sutural bone surface and blood vessel cells, were counted within 6 randomly selected grid blocks, each with a standardized size of 110 × 110 μm^2 under 20× magnification. The average osteoblast surface was measured by calculating the percentage of sutural bone surface resided by mononucleated, cuboidal cells by computerized histomorphometric analysis. The average sutural bone interface occupied by osteoclast-like cells, i.e., those multinucleated cells with at least 3 distinctive nuclei, was also measured by computerized histomorphometric analysis.

Statistical analysis

Control and cyclic loading groups were compared with regard to the average geometric widths, sutural cell density, osteoblast surface and osteoclast surface at each of P17, P23, and P32 using the Analysis of Variance (ANOVA) with Bonferroni tests at an alpha level of 0.05.

Results

Cyclic loading

A representative trace of cyclic force applied to the rat maxilla and recorded with a load cell is demonstrated in Fig. 1C. Compressive forces, negative in polarity, oscillated at 4 Hz and peaked at approximately 300 mN, as shown in the representative 6 s time course. The total cycles of force oscillation were 4800 cycles per day (c.p.d.) over 5 consecutive days. Application of cyclic loading in the animal model was uneventful and resulted in consistent loading patterns over time, as in our previous studies of cyclic loading in both the rat and rabbit models [4,18,19,25,26].

Suture geometric changes

The complex geometry of the suture was measured by a histomorphometric approach to construct circles that bisect the width of the cranial suture at multiple locations defined by grid blocks, as shown in Fig. 1D. This approach yielded reproducible data in our previous work on both cranial sutures and cranial base growth plate [4,25,26]. Representative photomicrographs of H&E-stained sections of the control PMS are demonstrated in Figs. 2A–C, whereas corresponding cyclic loading groups of the PMS are shown in Figs. 2A′–C′. In the control PMS at P17, P23 and P32 (Figs. 2A–C, respectively), the boundary of bone (b)

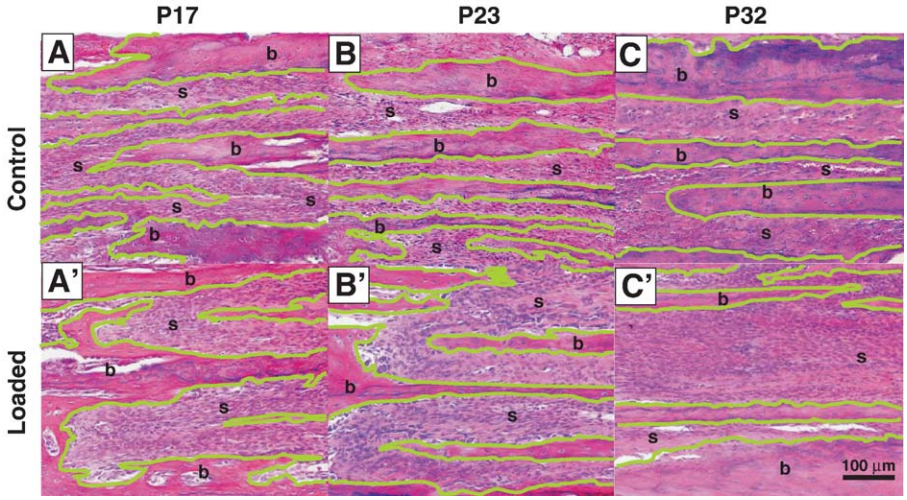

Fig. 2. Representative photomicrographs of the control and cyclically loaded rat premaxillomaxillary sutures (PMS) at 17, 23, and 32 days of postnatal life. The PMS at each of P17 (A), P23 (B), and P32 (C) is highly interdigitated with islands of bone (b) interfacing with suture (s). The interface between suture and bone is traced in green to assist visual identification. In comparison with relatively uniform sutural widths associated with control specimens (A–C), cyclic loading apparently increased the sutural width for P17 (A′), P23 (B′), and P32 (C′) relative to corresponding controls. The sutural width upon cyclic loading appears to be more variable. These qualitative impressions are confirmed by quantitative sutural width measurements in Fig. 4A.

and suture (s) was readily identified. The zig-zag course of the PMS was evident (Figs. 2A–C). In the cyclic loading group at each of P17, P23 and P32 (Figs. 2A′–C′), although the boundary between suture and bone remained evident, the geometric width of the sutures qualitatively increased, in comparison with corresponding controls (Figs. 2A–C). Computerized histomorphometric analysis revealed that the average sutural widths of the control PMS at P17, P23, and P32 were 65 ± 7 μm, 66 ± 8 μm, and 107 ± 14 μm (Fig. 4A). Upon cyclic loading, the average PMS widths increased to 86 ± 7 μm, 99 ± 12 μm, and 149 ± 30 μm, representing statistically significant increases by 32%, 50%, and 39% for P17, P23, and P32, respectively (Fig. 4A).

Similar morphological and morphometric changes were identified in the NFS, although certain interesting characteristics of the NFS differed from those of the PMS. In the control NFS at each of P17, P23, and P32, the zig-zag course of the suture was identified as regular strips of interfacing suture (s) and bone (b) (Figs. 3A–C). In comparison, the regular course of the NFS was altered by cyclic loading, especially in the P17 and P23 samples (Figs. 3A′ and B′). The qualitative increases in the sutural width of the NFS upon cyclic loading (Figs. 3A′–C′) were substantiated by significantly higher average sutural width in association with cyclic loading at P17, P23 and P32 than corresponding controls (Fig. 4B). The average geometric width of the NFS was 66 ± 5 μm, 74 ± 4 μm, and 74 ± 7 μm for P17, P23 and P32, respectively (Fig. 4B). In the cyclic loading group, the average NFS widths increased significantly to 88 ± 15 μm, 92 ± 10 μm, and 100 ± 14 μm for P17, P23, and P32, representing 33%, 24% and 32% increases relative to age-matched controls (Fig. 4B). In both the control and cyclically loaded PMS and NFS specimens, the boundary between suture and bone was evident (Figs. 2 and 3). There was a lack of microcracks or microfracture in response to cyclic loading by qualitative observations.

Sutural cell count, osteoblast surface and osteoclast surface

The number of cells present in each suture, excluding blood vessel cells and osteogenic lineage cells lining sutural bone surface, was counted in randomly selected, standardized grids. The average suture cell density of the control PMS was 6281 ± 1058, 7240 ± 529, and 7339 ± 66 cells/mm^2 for P17, P23, and P32, respectively (Fig. 4C). Upon cyclic loading, the average sutural cell density of the PMS increased to 10182 ± 132, 9752 ± 661, and 9521 ± 628 cells/mm^2 for P17, P23, and P32, respectively ($P < 0.01$) (Fig. 4C). These quantitative increases in cell density of the PMS are further evidenced by photomicrographic images of the control PMS (Figs. 5A–C), in comparison with increased cell density upon cyclic loading (Figs. 5A′–C′). Similarly, the average cell density of the NFS upon cyclic loading at 9884 ± 893, 9818 ± 1091, and 9355 ± 661 cells/mm^2 for P17, P23, and P32, respectively, was significantly higher than the average sutural cell density of the corresponding control NFS at 6876 ± 66, 6744 ± 264, and 6678 ± 397 cells/mm^2 ($P < 0.01$) (Fig. 4D). These quantitative increases in cell density of the PMS are further evidenced by photomicrographic images of the control NFS (Figs. 6A–C), in comparison with increased cell density of the NFS upon cyclic loading (Figs. 6A′–C′). In many instances, such as those demonstrated in Figs. 5 and 6, cyclic loading apparently was associated with more rounded shape of sutural cells, especially at P17 and P23 (Figs. 5A′, B′ and 6A′, B′) in comparison with the spindle shape of sutural cells in the control groups at P17 and P23 (Figs. 5A, B and 6A, B).

The sutural bone surface resided by mononucleated, cuboidal cells in the control PMS, excluding flat, mononucleated bone

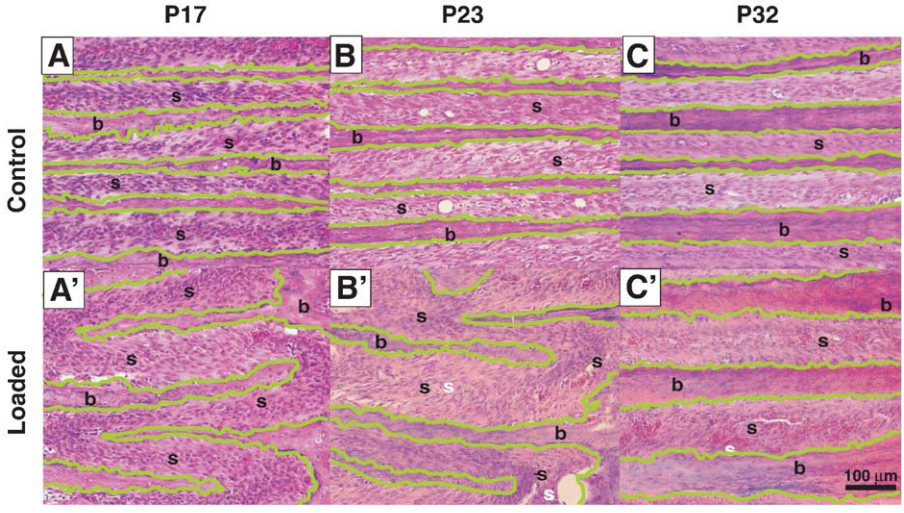

Fig. 3. Representative photomicrographs of the control and cyclically loaded rat nasofrontal sutures (NFS) at 17, 23, and 32 days of postnatal life. The NFS at each of P17 (A), P23 (B), and P32 (C) is highly interdigitated with islands of bone (b) interfacing with suture (s). The interface between suture and bone is traced in green color to assist visual identification. In comparison with relatively uniform sutural widths associated with control specimens (A–C), cyclic loading apparently increased the sutural width for P17 (A′), P23 (B′), and P32 (C′) relative to corresponding controls. The sutural width upon cyclic loading appears to be more variable. These qualitative impressions are confirmed by quantitative sutural width measurements in Fig. 4B.

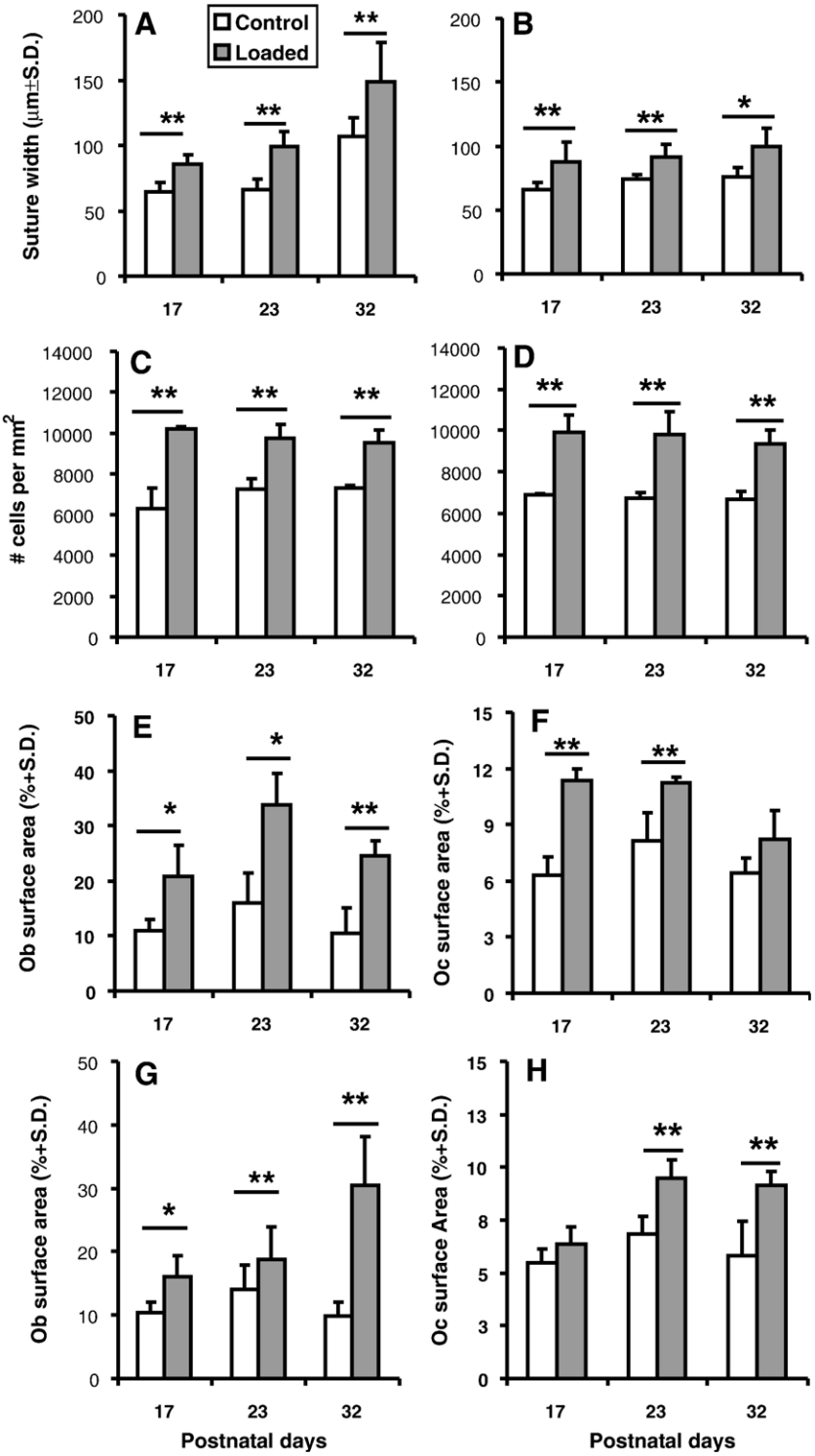

Fig. 4. Quantification of histomorphometric data at 17, 23 and 32 postnatal days (P17, P23, and P32) of the control (open bars) and cyclic loading (solid bars) groups. (A) The average width of the rat premaxillomaxillary sutures (PMS) upon cyclic loading is significantly higher than corresponding controls at each of P1, P23 and P32. (B) The average width of the rat nasofrontal sutures (NFS) at each of P17, P23 and P32 upon cyclic loading is significantly higher than corresponding controls. (C) The average cell density of the PMS at each of P17, P23 and P32 upon cyclic loading is significantly higher than corresponding controls. (D) The average cell density of the NFS at each of P17, P23 and P32 is significantly higher than corresponding controls. (E) The average sutural bone surface resided by mononucleated, cuboidal osteoblast-like cells (Ob) of the PMS at each of P17, P23 and P32 is significantly higher than corresponding controls. (F) The average sutural bone surface resided by multinucleated osteoclast-like cells (Oc) of the PMS at each of P17 and P23 upon cyclic loading is significantly higher than corresponding controls, but not P32. (G) The average sutural bone surface resided by osteoblast-like cells of the NFS at each of P17, P23 and P32 upon cyclic loading is significantly higher than corresponding controls. (H) The average sutural bone surface resided by osteoclast-like cells of the NFS at each of P23 and P32 upon cyclic loading is significantly higher than corresponding controls, but not P17. Ob: osteoblasts; Oc: osteoclasts; $N = 6–7$ per group. *$P < 0.05$; **$P < 0.01$.

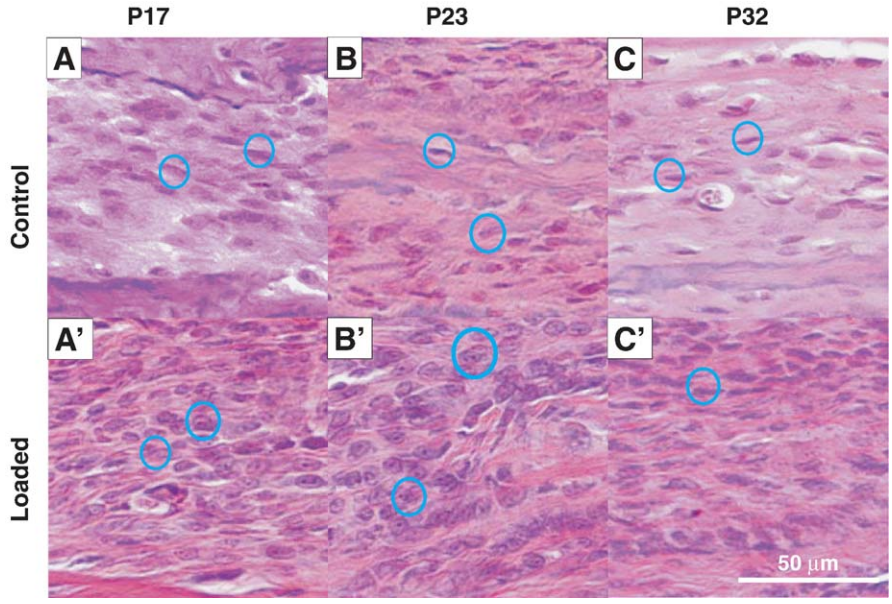

Fig. 5. Cell density of representative photomicrographs of the control and cyclically loaded rat premaxillomaxillary sutures (PMS) at 17, 23, and 32 days of postnatal life. Cells in suture mesenchyme were counted, with exclusion of osteogenic lineage cells lining the sutural bone surface and blood vessel cells. Representative sutural cells are identified with blue circles. The postnatal PMS at each of P17 (A), P23 (B), and P32 (C) has abundant fibroblast-like cells. In comparison, cell density apparently has increased upon cyclic loading for P17 (A′), P23 (B′), and P32 (C′) relative to corresponding controls. In some cases, sutural cells apparently become more cuboidal, as opposed to the spindle-like shape in controls.

lining cells, was 10.97 ± 2.04%, 15.91 ± 5.57%, and 10.54 ± 4.68% for P17, P23, and P32, respectively (Fig. 4E). Cyclic loading increased the average osteoblast surface of the PMS to 20.76 ± 5.8%, 33.90 ± 6.17%, and 24.55 ± 4.68% for P17, P23, and P32, respectively (Fig. 4E). In contrast, the average sutural surface occupied by multinucleated osteoclasts of the control PMS was 6.34 ± 0.67%, 8.16 ± 1.45%, and 6.43 ± 0.77% for P17, P23, and P32, respectively (Fig. 4F). Upon cyclic loading, the average sutural osteoclast surface of the PMS was 11.37 ± 0.95%, 11.21 ± 1.45%, and 8.19 ± 0.77% for P17, P23, and P32, respectively (Fig. 4E). For the NFS, the average sutural osteoblast surface for P17, P23, and P32 of the

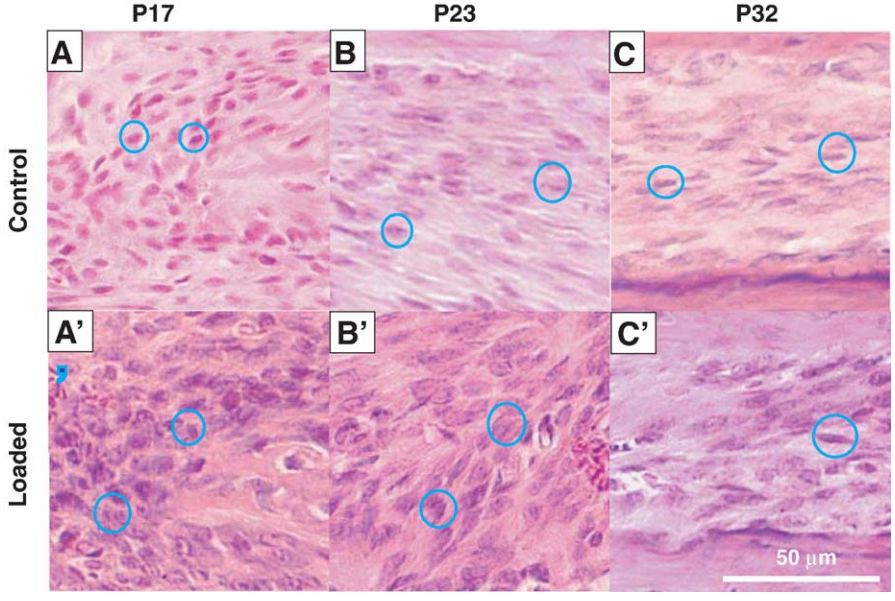

Fig. 6. Cell density of representative photomicrographs of the control and cyclically loaded rat nasofrontal sutures (NFS) at 17, 23, and 32 days of postnatal life. Cells in suture mesenchyme were counted, with exclusion of osteogenic lineage cells lining the sutural bone surface and blood vessel cells. Representative sutural cells are identified with blue circles. The postnatal PMS at each of P17 (A), P23 (B), and P32 (C) has abundant fibroblast-like cells. In comparison, cell density apparently has increased upon cyclic loading for P17 (A′), P23 (B′), and P32 (C′) relative to corresponding controls. In some cases, sutural cells apparently become more cuboidal, as opposed to the spindle-like shape in controls.

control group was 10.32 ± 1.80%, 14.05 ± 3.79%, and 9.80 ± 2.17% for P17, P23, and P32, respectively (Fig. 4G). Cyclic loading increased the average NFS osteoblast surface to 16.09 ± 3.33%, 18.83 ± 5.1%, and 30.41 ± 7.65% for P17, P23, and P32, respectively (Fig. 4G). In comparison, the average NFS osteoclast surface for P17, P23 and P32 was 5.45 ± 0.67%, 6.83 ± 0.84%, and 5.82 ± 1.64% for P17, P23, and P32, respectively (Fig. 4H). Cyclic loading increased the average NFS sutural osteoclast surface to 6.34 ± 0.81 9.45 ± 0.88, and 7.13 ± 0.69%, respectively (Fig. 4H). Statistical comparison revealed that osteoblast-occupied sutural surface was significantly greater in cyclically loaded sutures at P17, P23, and P32 than corresponding controls for both the PMS and NFS sutures (Figs. 4E and G). However, cyclic loading elicited significantly higher sutural bone surface populated by osteoclast-like cells for P17 and P23, but not P32, for the PMS (Fig. 4F). For the NFS, sutural osteoclast surface was significantly higher upon cyclic loading for P23 and P32 days, but not P17 (Fig. 4H).

Discussion

The present data suggest that a short dose of cyclic loading with a peak-to-peak magnitude of 300 mN is capable of modulating cellular and morphological growth responses of cranial sutures at the postnatal stage. The present data, derived from a postnatal rat model, are consistent with our previous findings of mechanical modulation of sutural growth based on the juvenile rabbit model [4,13]. The present experimental paradigm utilizes cyclic loading at 4 Hz, in comparison with 1 Hz in [4], but with a reduced force magnitude at 300 mN from 5 N as in [4]. The present observation of elevated sutural growth responses by cyclic forces at a higher frequency (4 Hz), in comparison with our previous work, appears to suggest that sutural cells are responsive to a multitude of force frequencies. In the present study, both sutural width and sutural cell density are significantly higher upon cyclic loading than controls corresponding controls.

Suture growth is characterized by several parallel events such as increases in sutural width, sutural cell density and sutural osteogenesis [1–3]. Each event is complex and accounted for by interactions between multiple cell lineages such as mesenchymal cells, fibroblast-like cells and osteogenic cells among other cell types [1,2]. Increases in sutural width upon mechanical loading may be analogous to increases in growth plate height of the cranial base [25,26], and has been observed in our previous work in juvenile rabbits upon the application of brief doses of mechanical forces at 0.25 Hz and 1 Hz [4,13]. The present increases in sutural width are of even greater magnitude, likely accounted for by several factors such as the higher force frequency at 4 Hz, and perhaps rapid craniofacial growth potential in the neonatal age [18,27]. Increases in sutural width may have resulted from increased fibrogenesis in suture mesenchyme among other factors [4]. Alternatively, it is conceivable that both sutural fibrogenesis and osteogenesis are enhanced by cyclic loading, but sutural fibrogenesis is increased to a greater extent, with a net result of increased sutural width. In two parallel studies, cyclic loading at 4 Hz upregulates metalloproteinase-1 and/or-2 genes in several cranial and facial sutures of postnatal rats [18,19], suggesting the potential involvement of MMP-coded proteinases such as collagenase in sutural modeling and/or remodeling. Another direct evidence for sutural remodeling and/or remodeling is the presently observed increases in the sutural bone surface resided by multinucleated osteoclast-like cells. Although osteoclast-mediated bone resorption may seem to be contradictory to the net result of rapid sutural growth in the postnatal age, it is perhaps necessary for sutures to change morphological characteristics.

Sutural cell density increases as a result of cyclic loading in all 3 age groups of P17, P23, and P32. The present cell count excludes blood vessel cells and cells aligning the sutural bone surface, i.e., both osteoblasts and bone lining cells. Thus, the presently observed increases in sutural cell density suggests that cells in suture mesenchyme, likely including mesenchymal cells and fibroblast-like cells, increase their proliferation rates and/or decrease their apoptotic rates upon the application mechanical stress. The apoptosis rate of sutural fibroblasts is significantly higher in the synostosed rat posterior interfrontal suture than the patent sagittal suture [28]. However, little is known whether mechanical stress alters the apoptosis rate of sutural cells. Apoptosis markers and mitotic cell labeling are necessary, for example by using bromodeoxyuridine (BrdU), to differentiate between increasing proliferation and decreasing apoptotic rate. Cranial sutures contain two distinct cell populations: cells producing un-mineralized type I collagen in the center of the suture, and cells producing to-be-mineralized type I collagen that becomes sutural bone. Whereas the latter clearly is the osteoblast lineage which has been excluded from the present cell density counting, the precise nature of the former, i.e., cells producing type I collagen in the center of the suture without subsequent mineralization, is somewhat uncertain. Some believe that the majority of the cells residing in the center of the suture are mesenchymal cells [29]. Accordingly, the tissue in the center of the suture is referred to as ‘suture mesenchyme’, especially among developmental biologists e.g. [7,29]. Since type I collagen is the most abundant collagen phenotype in cranial and facial sutures [14,30–33], cranial sutures must contain cells that produce type I collagen fibrils, which then aggregate into collagen fibers in the extracellular matrix without subsequent mineralization. Although in all likelihood, sutures contain mesenchymal cells, the progenitor status of mesenchymal cells nullifies the possibility that their main function is to synthesize a substantial amount of type I collagen fibrils [34]. Due to this general constraint of a lack of characterization of different lineages of sutural cells, the present data of sutural cell density should be interpreted with the caution that all cell lineages in suture mesenchyme, excluding blood vessel cells and sutural osteogenic lineage cells, are represented. Another important issue is whether the increases in cell density is temporary or have impact on bone apposition and/or remodeling. In [37], we observed parallel increases in BV/TV and the number of osteoblasts that line the endocortical bone surface. However, whether this represents a direct cause–effect relationship warrants additional investigations.

Within the constraint of the present approaches, the present data of sutural width and sutural cell density in neonatal rats provide the needed baseline information of the development and mechanical modulation of early postnatal craniofacial sutures. Despite recent report of sutural development in growing animals [3,4], the present data are valuable in the understanding of sutural development in the early postnatal stage that is characterized by rapid cell lineage changes and matrix synthesis. The present neonatal age likely represents more active sutural growth stage than the growing animals in [4]. This study may also have potential implications in formulating new concepts in devising innovative orthodontics and craniofacial orthopedic appliances in consideration that only static forces have been employed in the correction of craniofacial disfigurations [35,36]. Although certain perturbation is superimposed to static forces applied in orthodontic tooth movement and distraction osteogenesis from functional activities such as mastication and respiration, these perturbations are unlikely in the same magnitude and frequency of the cyclic forces applied in this study. The present data demonstrate that cyclic forces are potent stimuli for modulating sutural growth in neonatal rats. Combined analysis with our previous data in the juvenile rabbit model demonstrates that sutural cells retain the capacity to respond to mechanical stress during active physical growth.

Acknowledgments

Aurora Lopez is gratefully acknowledged for general technical assistance. We thank two anonymous reviewers whose highly meritorious suggestions helped improve the quality of the manuscript. This research was supported by NIH grants DE13964 and DE15391.

References

[1] Opperman LA. Cranial sutures as intramembranous bone growth sites. Dev Dyn 2000;219:472–85.
[2] Mao JJ. Mechanobiology of craniofacial sutures. J Dent Res 2002; 81:810–6.
[3] Mao JJ. Mechanics and mesenchymal cells in craniofacial development. Curr Opin Orthop 2005;16:331–7.
[4] Kopher RA, Mao JJ. Suture growth modulated by the oscillatory component of micromechanical strain. J Bone Miner Res 2003;18: 521–8.
[5] Vastardis H, Mulliken JB, Glowacki J. Unilateral coronal synostosis: a histomorphometric study. Cleft Palate Craniofac J 2004;41:439–46.
[6] Orestes-Cardoso SM, Nefussi JR, Hotton D, Mesbah M, Orestes-Cardoso MD, Robert B, et al. Postnatal Msx1 expression pattern in craniofacial, axial, and appendicular skeleton of transgenic mice from the first week until the second year. Dev Dyn 2001;221:1–13.
[7] Rice DP, Kim HJ, Thesleff I. Apoptosis in murine calvarial bone and suture development. Eur J Oral Sci 1999;107:265–75.
[8] Winograd JM, Im MJ, Vander C, Kolk A. Osteoblastic and osteoclastic activation in coronal sutures undergoing fusion ex vivo. Plast Reconstr Surg 1997;100:1103–12.
[9] Selman AJ, Sarnat BG. Growth of the rabbit snout after extirpation of the frontonasal suture: a gross and serial roentgenographic study by means of metallic implants. Am J Anat 1957;101:273–93.
[10] Sarnat BG. Gross growth and regrowth of sutures: reflections on some personal research. J Craniofac Surg 2003;14:438–44.
[11] Herring SW. Sutures—A tool in functional cranial analysis. Acta Anat 1972;83:222–47.
[12] Jaslow CR. Mechanical properties of cranial sutures. J Biomech 1990;23:313–21.
[13] Mao JJ, Wang X, Mooney MP, Kopher RA, Nudera JA. Strain induced osteogenesis of the craniofacial suture upon controlled delivery of low-frequency cyclic forces. Front Biosci 2003;8:a10–7.
[14] Rafferty KL, Herring SW. Craniofacial sutures: morphology, growth, and in vivo masticatory strains. J Morphol 1999;242:167–79.
[15] Sun Z, Lee E, Herring SW. Cranial sutures and bones: growth and fusion in relation to masticatory strain. Anat Rec A Discov Mol Cell Evol Biol 2004;276:150–61.
[16] Kopher RA, Nudera JA, Wang X, O'Grady K, Mao JJ. Expression of in vivo mechanical strain upon different wave forms of exogenous forces in rabbit craniofacial sutures. Ann Biomed Eng 2003; 31:1125–31.
[17] Green DD, Hembry RM, Atkinson SJ, Reynolds JJ, Meikle MC. Immunolocalization of collagenase and tissue inhibitor of metalloproteinases (TIMP) in mechanically deformed fibrous joints. Am J Orthod 1990;97:281–8.
[18] Collins JM, Ramamoorthy K, Da Silveira A, Patston PA, Mao JJ. Microstrain in intramembranous bones induces altered gene expression of MMP1 and MMP2 in the rat. J Biomech 2005;38:485–92.
[19] Almubarak R, Da Silveira A, Mao JJ. Expression of matrix metalloproteinase genes 1 and 2 in rat facial and cranial sutures. Cell Tissue Res 2005;321:465–71.
[20] Hillam RA, Skerry TM. Inhibition of bone resorption and stimulation of formation by mechanical loading of the modeling rat ulna in vivo. J Bone Miner Res 1995;10:683–9.
[21] Mosley JR, Lanyon LE. Strain rate as a controlling influence on adaptive modeling in response to dynamic loading of the ulna in growing male rats. Bone 1998;23:313–8.
[22] Fritton SP, McLeod KJ, Rubin CT. Quantifying the strain history of bone: spatial uniformity and self-similarity of low-magnitude strains. J Biomech 2000;33:317–25.
[23] Schriefer JL, Warden SJ, Saxon LK, Robling AG, Turner CH. Cellular accommodation and the response of bone to mechanical loading. J Biomech 2005;1838:38–45.
[24] Turner CH, Robling AG. Mechanisms by which exercise improves bone strength. J Bone Miner Metab 2005;23:16–22 [Suppl].
[25] Wang X, Mao JJ. Accelerated chondrogenesis of the rabbit cranial base growth plate by oscillatory mechanical stimuli. J Bone Miner Res 2002;17:1843–50.
[26] Wang X, Mao JJ. Chondrocyte proliferation of the cranial base cartilage upon vivo mechanical stresses. J Dent Res 2002;81:701–5.
[27] Moss ML. Growth of the calvaria in the rat. Am J Anat 1954; 94:333–61.
[28] Fong KD, Warren SM, Loboa EG, Henderson JH, Fang TD, Cowan CM, et al. Mechanical strain affects dura mater biological processes: implications for immature calvarial healing. Plast Reconstr Surg 2003;112:1312–27.
[29] Morriss-Kay GM. Derivation of the mammalian skull vault. J Anat 2001;199:143–51.
[30] Meikle MC, Heath JK, Reynolds JJ. The use of in vitro models for investigating the response of fibrous joints to tensile mechanical stress. Am J Orthod 1984;85:141–53.
[31] Takahashi I, Mizoguchi I, Nakamura M, Sasano Y, Saitoh S, Kagayama M, et al. Effects of expansive force on the differentiation of midpalatal suture cartilage in rats. Bone 1996;18:341–8.
[32] Zimmerman B, Moegelin A, de Souza P, Bier J. Morphology of the development of the sagittal suture of mice. Anat Embryol (Berl) 1998;197:155–65.
[33] Cohen Jr MM. Merging the old skeletal biology with the new: II. Molecular aspects of bone formation and bone growth. J Craniofac Genet Dev Biol 2000;20:94–106.
[34] Alhadlaq A, Mao JJ. Mesenchymal stem cells: isolation and therapeutics. Stem Cells Dev 2004;13:436–48.

[35] Graber TM, Vanarsdall Jr RL. Orthodontics: current principles and techniques. 2nd ed. St. Louis, MO: Mosby; 1994. p. 193–234.
[36] Proffit WR, Fields HW, Ackerman JL, Sinclair PM, Thomas PM, Tulloch JFC. Contemporary orthodontics. St. Louis, MO: Mosby; 2000. p. 271–94.
[37] Clark PA, Rodriguez A, Sumner DR, Hussain MA, Mao JJ. Modulation of bone ingrowth of rabbit femur titanium implants by in vivo axial micromechanical loading. J Appl Physiol 2005;98:1922–9.
[38] Herring SW, Rafferty KL, Liu ZJ, Marshall CD. Jaw muscles and the skull in mammals: the biomechanics of mastication. Comp Biochem Physiol A Mol Integr Physiol 2001;131:207–19.